Supporting Information for

Bioimaging, Cellular Uptake and Dynamics in Living Cells of a Lipophilic Fluorescent Benzothiadiazole at Low Temperature (4 °C)

Alberto A. R. Mota,[a] Pedro H. P. R. Carvalho,[a] Bruna C. Guido,[a] Heibbe C. B. de Oliveira,[a] Thereza A. Soares,[b] José R. Corrêa,[a] and Brenno A. D. Neto,*[a]

brenno.ipi@gmail.com

[a] Laboratory of Medicinal and Technological Chemistry, University of Brasilia (IQ-UnB). Campus Universitario Darcy Ribeiro, CEP 70904970, P.O.Box 4478, Brasilia-DF, Brazil.

[b] Department of Fundamental Chemistry, (dQF-UFPE), Av. Jornalista Anibal Fernandes, s/n – Cidade Universitaria, 50740-560, Recife-PE, Brazil.

DFT Calculations. Theoretical treatment of **BTD-AO** was performed using the density functional theory (DFT) approach of the Gaussian 09 series of programs.[1] Geometry optimization of the ground (S_0) and first excited (S_1) states (in gas phase and water) were conducted with 6-311G(d) Pople's split-valence basis set and hybrid exchange–correlation functional using the Coulomb-attenuating method (CAM-B3LYP).(2) Harmonic frequency calculations were performed verify whether we have located a genuine minimum. The optimized geometries of S_0 and S_1 were used for the single point TD-DFT calculation using different exchange-correlation (XC) functional (wB97XD, PBE1PBE, M062X, CAM-B3LYP, B3LYP and B2PLYP) in combination with 6-311+G(2d,p). In particular, absorption spectra in close agreement with experiments have been obtained using the TD-PBE1PBE/6-311+G(2d,p) level of calculation.[2, 3] To include the solvent effects in our quantum mechanics calculations we have employed the self-consistent reaction field (SCRF) approach with the polarizable continuum model (PCM)[4-6] were the solute molecule is enclosed in a cavity embedded in a dielectric medium.

Molecular docking. The crystallographic structure of albumin (PDB ID 1BJ5)[7] and the NMR structure of FAPB (PDB ID 2FLJ)[8] were used as initial coordinates for the molecular docking calculations of BTD-AO. Five molecules of myristic acid bound to albumin were removed before the molecular docking calculations. Likewise for the oleic acid molecule bout to FAPB. During the conformational search the ligands were fully flexible concerning its degrees of translation, orientation and conformation with respect to the protein structure, which was kept rigid. Each sampled conformation was evaluated and ranked according to the empirical energy function (equation 2). Grid maps with 126 X 126 X 126 points of dimension were calculated using AutoGrid4.[9] Coarse (grid-point spacing of 0.25 Å) and fine (grid-point spacing of 0.14 Å) sets of grid maps were used during the docking simulations in order to sample the entire protein structure and ensure accurate estimates of host-guest interaction energies. Protonation states were assigned accordingly to pH 7. The partial charges on the protein atoms were taken from the AMBER all-atom force field.[10] The Lamarckian genetic algorithm as implemented in AutoDock4 program[11-13] was used with the following parameters: an initial population of 100 random individuals, a maximum number of 1.5 x 10^6 energy evaluations, a maximum number of 27000 generations with mutation and crossover rates of 0.02 and 0.08, respectively. An optional elitism parameter equal to 1 was applied, which determines the number of top individuals that will survive into the next generation. A maximum of 300 iterations per local search was allowed. The probability of performing a local search on an individual was 0.06 where the maximum number of consecutive successes or failures before doubling or halving the search step was 4. Ligand conformations presenting the most favorable binding energy were selected in each step of the simulation, in such a way that, at the end of calculation, atomic coordinates of the 200 conformers that better fitted the binding site were selected. These conformers were structurally compared through their RMSDs, and clustered into groups of similar conformations. A tolerance of 2 Å for RMSD was employed to assign conformers to the same cluster.

Cell imaging experiments. Cells were seed on coverslips at bottom of 24 wells plate and maintained on D-MEM medium (Sigma, MO - USA) supplemented with 10% of calf fetal serum at 37 °C in 5% CO_2 atmosphere. Staining procedures: The cells were separated on eight samples; all samples were incubated with 1mM of **BTD-AO**. Four samples at 4 °C and four samples at 37 °C were incubated for 5, 15, 30 min and 60 min for each sample. After the respective incubation condition, the samples were washed three times in phosphate buffer saline (PBS) at room temperature and fixed on formalin 3,7% for 30 min also at room temperature. No nucleus staining procedures was performed in order to check if there was any

probe affinity for the nuclei. The samples were washed three times in PBS and mounted on glass slides by using ProLong® Gold antifade reagents (Life Technologies, NY - USA). The cell images were acquired by using confocal laser scanning microscope TCS SP5 (Leica, IL-USA). Beside of regular images acquisition, it was also performed a stack images acquisition of 50 images and used to do a 3D image projection and orthogonal analysis in order to localize the probe inside. The orthogonal analyse was performed with the sample incubated for 60 min. All assays and tests were performed in triplicate. The nuclei were stained with propidium iodide using standard methods. Briefly, after incubation with **BTD-AO**, MCF-7, MDA-MB-231, Caco-2, and HeLa cells were equilibrated in 2X Saline-Sodium Citrate Buffer (SSC, 0.3 M NaCl, 0.03 M sodium citrate - pH 7.0), permeabilized in 2x SSC buffer with 100 μg/mL RNase-free DNase and 0.1% Triton-X100 for 20 minutes at 37 ° C and further washed three times (1 minute each) in 2X SSC. The samples were stained with propidium iodide (500 nM in 2 x SSC) for 7 minutes at room temperature, washed three times with 2 x SSC and the coverslips were mounted with ProLong Gold Antifade (Invitrogen - Life Technologies, Carlsbad, CA, USA). The specimens were observed and images were acquired under a laser scanning confocal microscope Leica SP 5 (Leica Microsystems - Wetzlar Germany).

Cell viability assays. Caco-2, MCF-7, MDA-MB-231, HeLa or HUVEC cells (3 x 10^3/well) were plated in 96 well plate. After adhesion the cells were washed twice with pre-warmed (37 °C) PBS and incubated in the buffer for 10 min at 37 °C. The samples were incubated with 1 mM of **BTD-AO** (diluted in DMEM (for Caco-2 and HeLa), RPMI (for MCF-7 and HUVEC) or L15 (for MDA-MB-231) culture medium supplemented with 10% FBS and 25 μg/mL gentamicin) for 1 h at 37 °C. The cytotoxicity was determined by using 3-(4,5-dimethylthiazol-2-yl)-2,5-diphenylterazolium bromide - known as MTT (Molecular Probes - Life Technologies, Carlsbad, CA, USA) - according to the manufacturer instructions. The absorbance readings were performed by spectrophotometer (SpectraMax M5, Molecular Devices - Sunnyvale, California, USA). Statistical analyses were performed using GraphPad Prism 5 Software and the statistical significance was determined by ANOVA with post-hoc comparison by Bonferroni test. A P value of <0.05 was considered statistically significant (*, $P < 0.05$; **$P < 0.01$ and ***$P < 0.001$).

NMR analyses. NMR spectra were recorded on a Varian Mercury Plus spectrometer 7.05 T (300 MHz for proton) at room temperature, using a 5-mm internal diameter probe. Deuterated chloroform ($CDCl_3$) and TMS (tetramethylsilane) were used as internal standards.

Mass spectrometry. ESI-QTOF-MS and MS/MS measurements were performed in the positive ion mode

(*m/z* 50-2000 range) on a Waters Synapt HDMS (Manchester, UK) instrument. This instrument has a hybrid quadrupole/ion mobility/orthogonal acceleration time-of-flight (oa-TOF) geometry and was used in the W mode, with the mobility cell switched off and working only as an ion guide. All samples were diluted in methanol with 0.1% formic acid to afford a 50 μM solution of **BTD-AO** and was directly infused into the ESI source at a flow rate of 10-20 μL/min. ESI source conditions were as follows: capillary voltage 3.0 kV, sample cone 10 to 30 V, extraction cone 3 V. Trap and Transfer cell collision energies were at 6 and 4 eV, respectively, Argon was used as CID gas in product ion spectrum experiments. The instrument was externally calibrated with phosphoric acid oligomers (H_3PO_4 0.05% v/v in H_2O/MeCN 50:50) from *m/z* 90 to 1000.

Synthesis of BTD-AO. 1.45 mmol of oleic acid (410 mg) was treated with $SOCl_2$ (5 mL) at reflux for 2 h. The thionyl chloride excess is then removed under vacuum. After, the commercially available 4-amino-2,1,3-benzothiadiazole (1.45 mmol, 220 mg) was added and heated at 130 °C for 30 min. Purification by column chromatography (EtOAc/hexane mixtures) gave the desired product in 61% yield.

^{1}H NMR (300 MHz, $CDCl_3$) δ (ppm) = 8.50 (dd, *J* = 7.3 Hz and 0.9 Hz, 1H), 8.46 (bs, 1H), 7.67 (dd, *J* = 8.5 and 1.2 Hz, 1H), 7.62-7.55 (m, 1H), 5.34 (m, 2H), 2.53 (t, *J* = 7.5 Hz, 2H), 2.01 (m, 4H), 1.80 (qui, *J* = 7.4 Hz, 2H), 1.36 (m, 20H), 0.87 (t, *J* = 7.2 Hz, 3H).

^{13}C NMR (APT) (75 MHz, $CDCl_3$) δ (ppm) = 171.8, 154.7, 147.7, 131.1, 130.0, 129.9, 129.7, 115.6, 114.8, 89.8, 37.9, 31.8, 29.7, 29.6, 29.5, 29.3, 29.2, 29.1(9), 29.1(0), 27.2, 27.1, 25.5, 22.6, 14.1.

Table S1. Selected theoretical calculated data for the dye **BTD-AO** in their ground and first excited state obtained from different exchange-correlation (*XC*) functional (wB97XD, PBE1PBE, M062X, CAM-B3LYP, B3LYP and B2PLYP) using the large 6-311+g(2d,p) Pople's split-valence basis. All results were obtained using the geometry fully optimized at CAM-B3LYP/6-311G(d) level of calculation.

XC	**State**	**μ(D)**		**HOMO(eV)**		**LUMO(eV)**		$\Delta E_{HOMO-LUMO}$**(eV)**		$\lambda_{abs}(nm)$	
		Gas	**Water**	**Gas**	**Water**	**Gas**	**Water**	**Gas**	**Water**	**Gas**	**Water**
B2PLYP	S_0	1.9736	3.0491	-7.168	-7.209	-1.284	-1.310	5.886	5.899	341.74	343.18
	S_1	2.4862	3.4578	-6.671	-6.730	-1.660	-1.715	5.010	5.014	-	-
B3LYP	S_0	1.9368	3.0588	-6.332	-6.358	-2.634	-2.644	3.698	3.714	394.21	394.62
	S_1	2.2225	3.3835	-5.960	-5.975	-2.971	-2.984	2.990	2.990	-	-
CAM-B3LYP	S_0	1.9763	3.1089	-7.664	-7.696	-1.496	-1.510	6.168	6.186	347.58	347.63
	S_1	2.2882	3.4559	-7.233	-7.249	-1.868	-1.895	5.364	5.355	-	-
M062X	S_0	2.0647	3.2418	-7.526	-7.587	-1.701	-1.734	5.824	5.853	340.79	340.40
	S_1	2.3759	3.5739	-7.079	-7.124	-2.078	-2.125	5.002	4.999	-	-
PBE1PBE	S_0	1.9477	3.0554	-6.526	-6.575	-2.477	-2.508	4.049	4.066	380.32	380.61
	S_1	4.8057	3.4053	-6.139	-6.177	-2.822	-2.860	3.316	3.317	-	-
wB97XD	S_0	1.9684	3.0940	-8.202	-8.251	-0.863	-0.894	7.339	7.357	344.33	344.98
	S_1	2.2852	3.4471	-7.775	-7.809	-1.233	-1.278	6.542	6.531	-	-

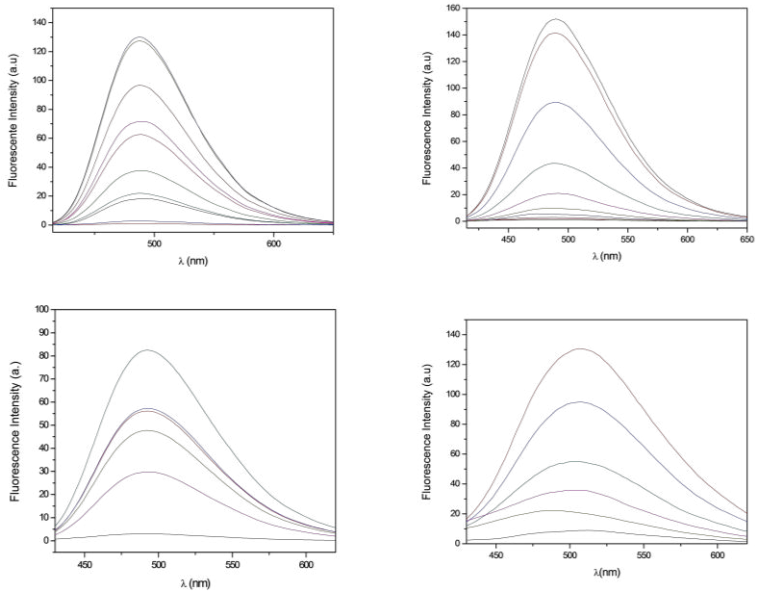

Figure S1. (Top, left) **BTD-AO** emission in acetonitrile (20 μM - 5 mM). (Top, right) **BTD-AO** emission in phosphate buffer (2 μM - 1 mM). (Bottom, right) **BTD-AO** emission in triton X100 solution (95 μM - 1 mM). (Bottom, right) **BTD-AO** emission in SDS solution (50 μM - 1 mM).

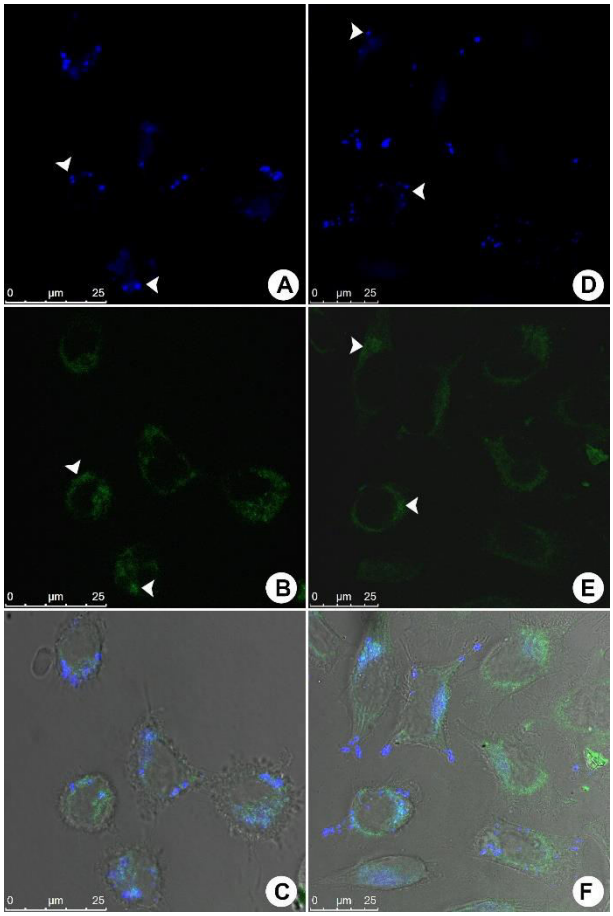

Figure S2. HeLa cells incubated with **BTD-AO** at 4 °C (A, B and C) and 37 °C (D, E and F) for 5 minutes. The probe accumulated on vesicles (lipid droplets) near to the peripheral region of the cells. The images show the same result for both temperatures tested as seen in (A), (B), (D) and (E) arrowheads. The blue fluorescent signal is seen in (A) and (D) whereas the green emission is seen in (B) and (E). (C) and (F) show the normal morphology of the cells by phase contrast microscopy. Scale bar of 25 µm.

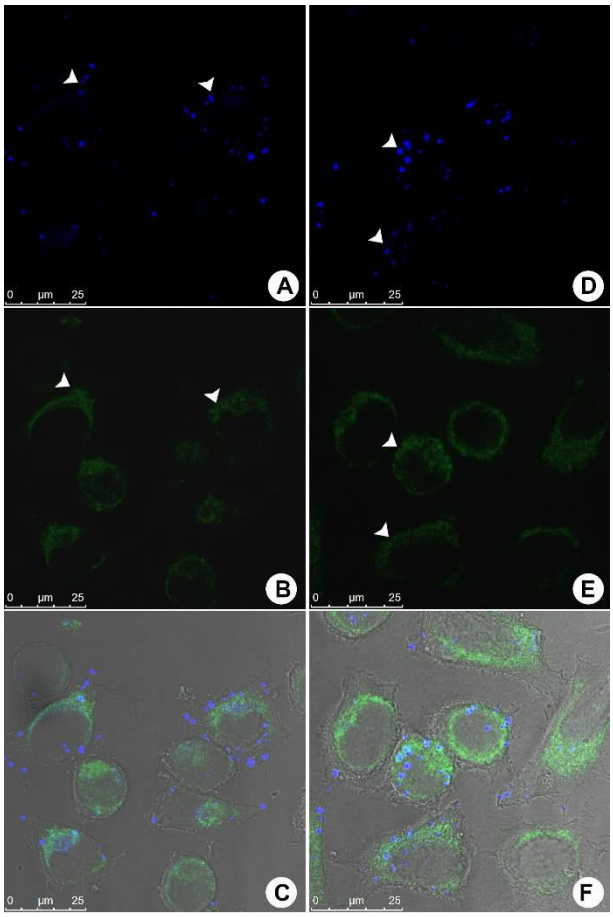

Figure S3. HeLa cells incubated with **BTD-AO** at 4 °C (A, B and C) and 37 °C (D, E and F) for 15 minutes. The probe accumulated on vesicles (lipid droplets) near to the peripheral region of the cells and at the inner position in the cells. The images show the same result for both temperatures tested as seen in (A), (B), (D) and (E) arrowheads. The blue fluorescent signal is seen in (A) and (D) whereas the green emission is seen in (B) and (E). (C) and (F) show the normal morphology of the cells by phase contrast microscopy. Scale bar of 25 µm.

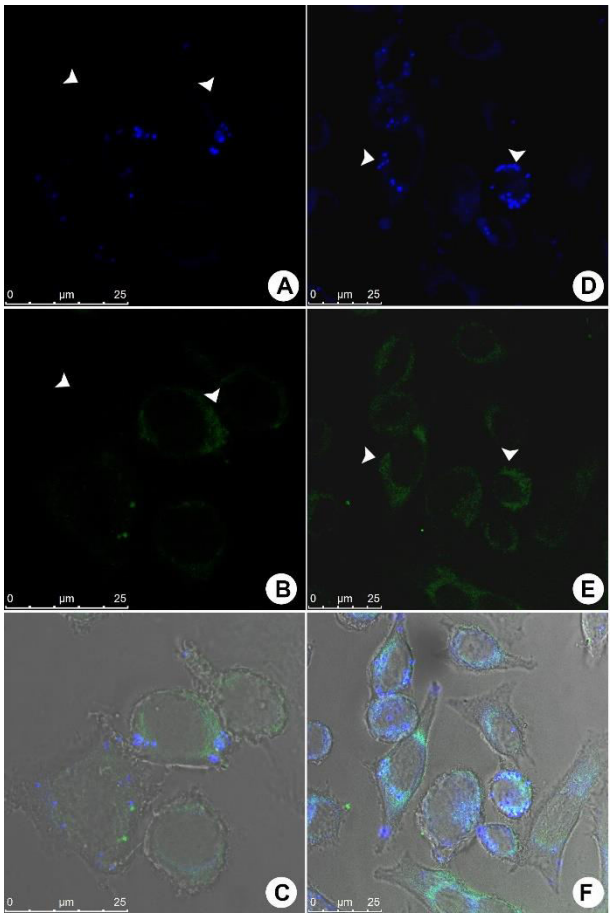

Figure S4. HeLa cells incubated with **BTD-AO** at 4 °C (A, B and C) and 37 °C (D, E and F) for 30 minutes. The probe accumulated on vesicles (lipid droplets) near to the peripheral region of the cells and at the inner position in the cells. The images show the same result for both temperatures tested as seen in (A), (B), (D) and (E) arrowheads. The blue fluorescent signal is seen in (A) and (D) whereas the green emission is seen in (B) and (E). (C) and (F) show the normal morphology of the cells by phase contrast microscopy. Scale bar of 25 µm.

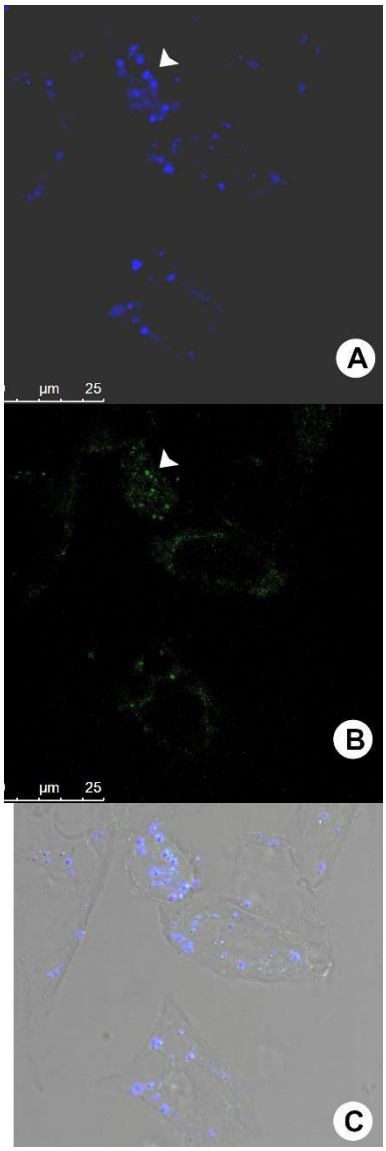

Figure S5. HeLa cells incubated with **BTD-AO** after 60 min. **BTD-AO** accumulated only inside the lipid droplets (vesicles) and only near to the cell nucleus. (A) Blue emission and (B) Green emission. (C) Shows the normal morphological aspects to these cells by phase contrast microscopy. Scale bar of 25 µm.

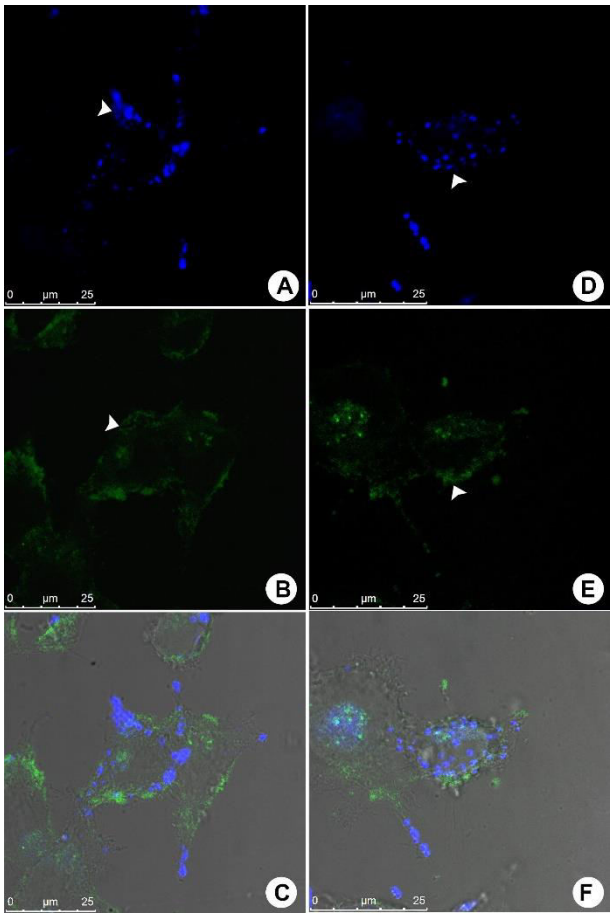

Figure S6. HUVEC cells (human umbilical vein/vascular endothelium cells) incubated with **BTD-AO** at 4 °C (A, B and C) and 37 °C (D, E and F) for 5 minutes. The probe accumulated on vesicles (lipid droplets) near to the peripheral region of the cells. The images show the same result for both temperatures tested as seen in (A), (B), (D) and (E) arrowheads. The blue fluorescent signal is seen in (A) and (D) whereas the green emission is seen in (B) and (E). (C) and (F) show the normal morphology of the cells by phase contrast microscopy. Scale bar of 25 µm.

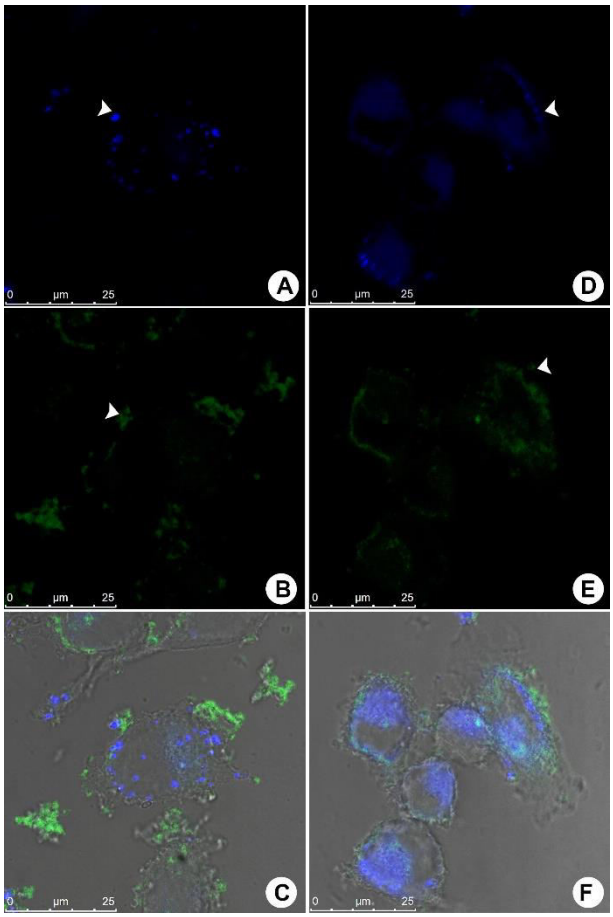

Figure S7. HUVEC cells (human umbilical vein/vascular endothelium cells) incubated with **BTD-AO** at 4 °C (A, B and C) and 37 °C (D, E and F) for 15 minutes. The probe accumulated on vesicles (lipid droplets) near to the peripheral region of the cells and at the inner position in the cells. The images show the same result for both temperatures tested as seen in (A), (B), (D) and (E) arrowheads. The blue fluorescent signal is seen in (A) and (D) whereas the green emission is seen in (B) and (E). (C) and (F) show the normal morphology of the cells by phase contrast microscopy. Scale bar of 25 µm.

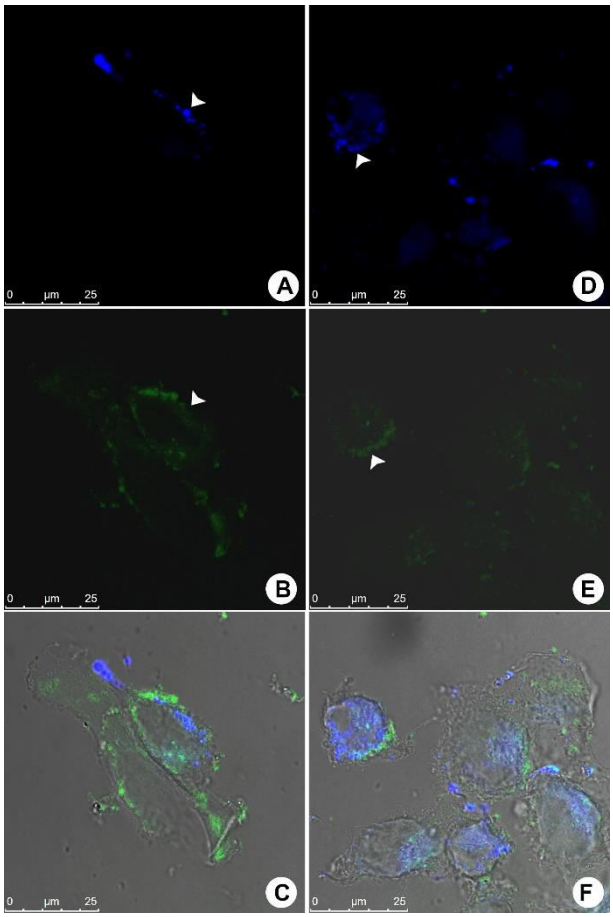

Figure S8. HUVEC cells (human umbilical vein/vascular endothelium cells) incubated with **BTD-AO** at 4 °C (A, B and C) and 37 °C (D, E and F) for 30 minutes. The probe accumulated on vesicles (lipid droplets) near to the peripheral region of the cells and at the inner position in the cells. The images show the same result for both temperatures tested as seen in (A), (B), (D) and (E) arrowheads. The blue fluorescent signal is seen in (A) and (D) whereas the green emission is seen in (B) and (E). (C) and (F) show the normal morphology of the cells by phase contrast microscopy. Scale bar of 25 µm.

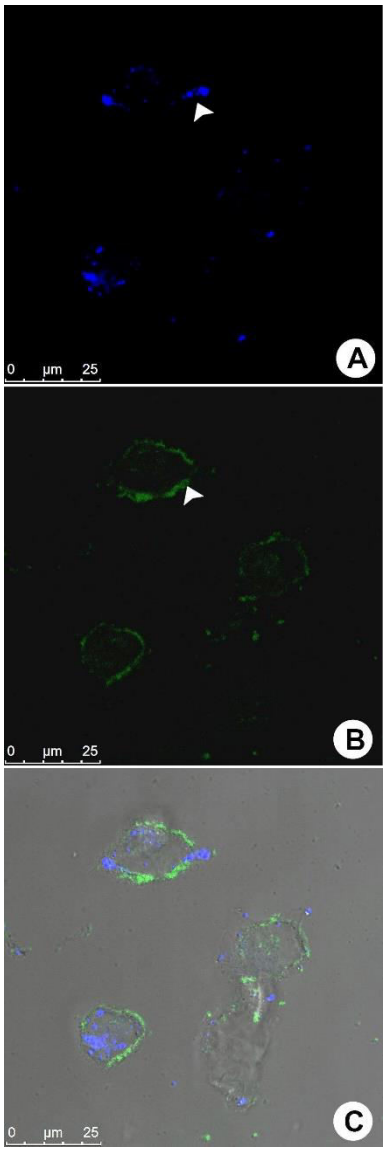

Figure S9. HUVEC cells (human umbilical vein/vascular endothelium cells) incubated with **BTD-AO** after 60 min. **BTD-AO** accumulated only inside the lipid droplets (vesicles) and only near to the cell nucleus. (A) Blue emission and (B) Green emission. (C) Shows the normal morphological aspects to these cells by phase contrast microscopy. Scale bar of 25 µm.

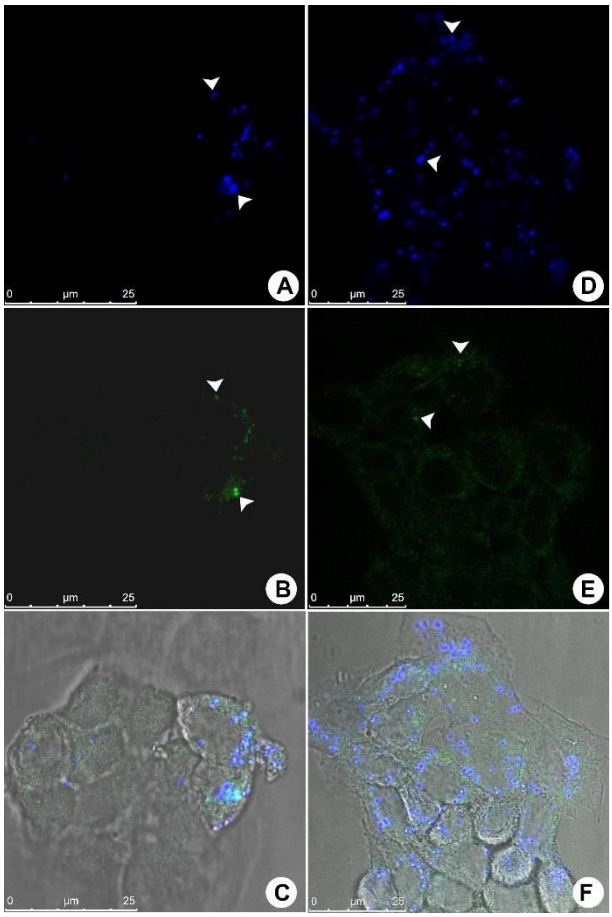

Figure S10. Caco2 cells (human colorectal adenocarcinoma cells) incubated with **BTD-AO** at 4 °C (A, B and C) and 37 °C (D, E and F) for 5 minutes. The probe accumulated on vesicles (lipid droplets) near to the peripheral region of the cells. The images show the same result for both temperatures tested as seen in (A), (B), (D) and (E) arrowheads. The blue fluorescent signal is seen in (A) and (D) whereas the green emission is seen in (B) and (E). (C) and (F) show the normal morphology of the cells by phase contrast microscopy. Scale bar of 25 µm.

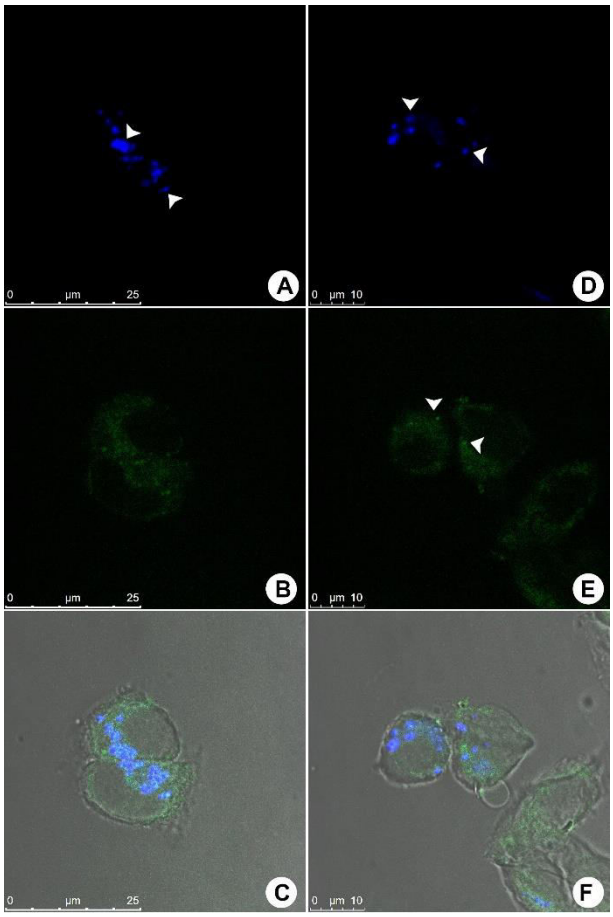

Figure S11. Caco2 cells (human colorectal adenocarcinoma cells) incubated with **BTD-AO** at 4 °C (A, B and C) and 37 °C (D, E and F) for 15 minutes. The probe accumulated on vesicles (lipid droplets) near to the peripheral region of the cells and at the inner position in the cells. The images show the same result for both temperatures tested as seen in (A), (B), (D) and (E) arrowheads. The blue fluorescent signal is seen in (A) and (D) whereas the green emission is seen in (B) and (E). (C) and (F) show the normal morphology of the cells by phase contrast microscopy. Scale bar of 25 µm.

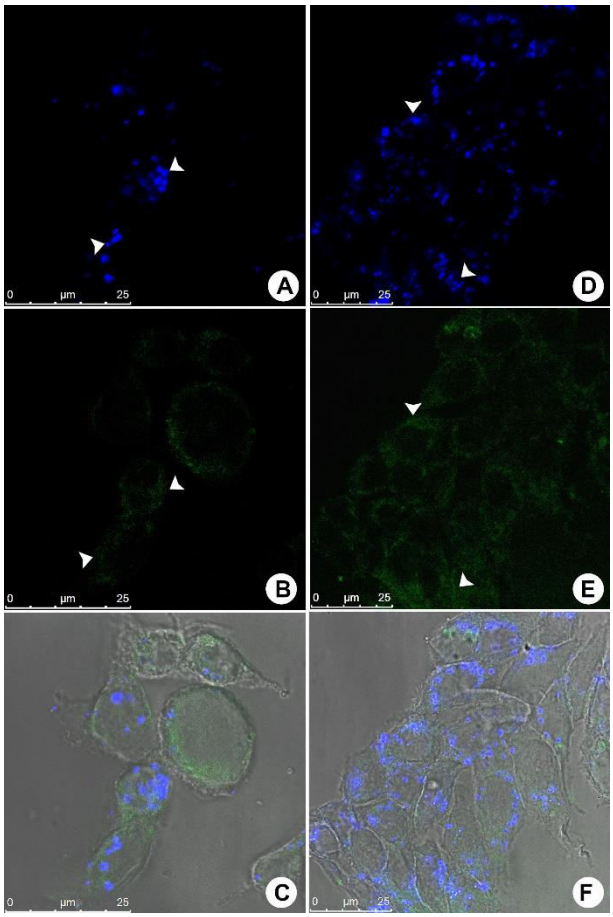

Figure S12. Caco2 cells (human colorectal adenocarcinoma cells) incubated with **BTD-AO** at 4 °C (A, B and C) and 37 °C (D, E and F) for 30 minutes. The probe accumulated on vesicles (lipid droplets) near to the peripheral region of the cells and at the inner position in the cells. The images show the same result for both temperatures tested as seen in (A), (B), (D) and (E) arrowheads. The blue fluorescent signal is seen in (A) and (D) whereas the green emission is seen in (B) and (E). (C) and (F) show the normal morphology of the cells by phase contrast microscopy. Scale bar of 25 µm.

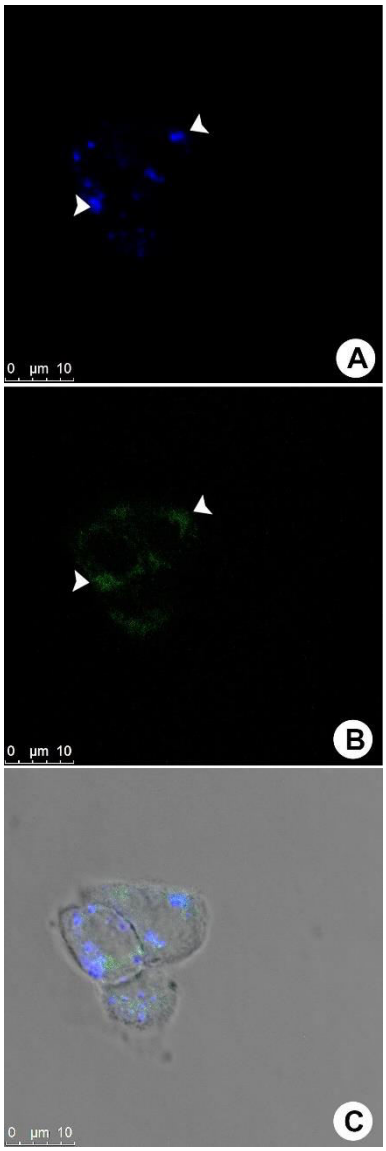

Figure S13. Caco2 cells (human colorectal adenocarcinoma cells) incubated with **BTD-AO** after 60 min. **BTD-AO** accumulated only inside the lipid droplets (vesicles) and only near to the cell nucleus. (A) Blue emission and (B) Green emission. (C) Shows the normal morphological aspects to these cells by phase contrast microscopy. Scale bar of 25 µm.

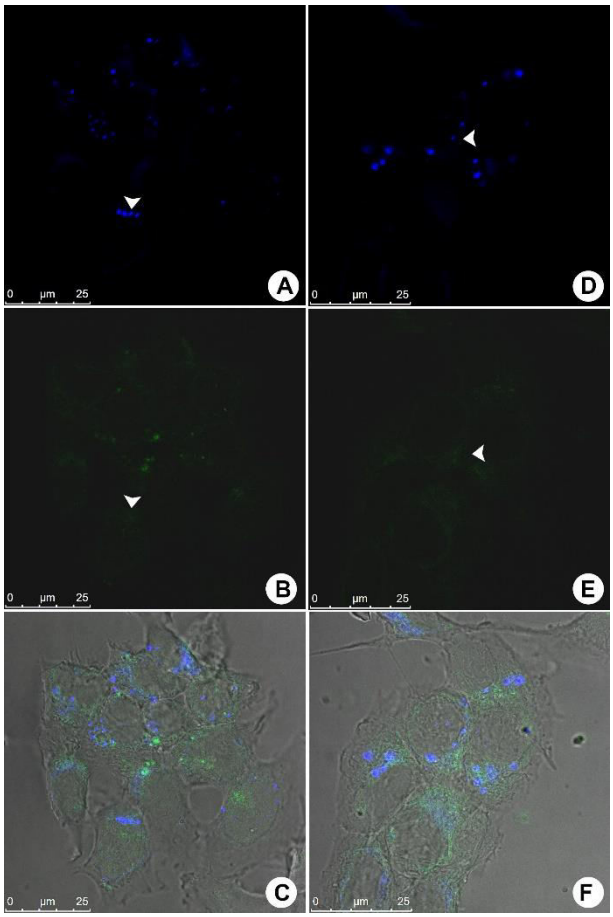

Figure S14. MCF-7 breast cancer cells incubated with **BTD-AO** at 4 °C (A, B and C) and 37 °C (D, E and F) for 5 minutes. The probe accumulated on vesicles (lipid droplets) near to the peripheral region of the cells. The images show the same result for both temperatures tested as seen in (A), (B), (D) and (E) arrowheads. The blue fluorescent signal is seen in (A) and (D) whereas the green emission is seen in (B) and (E). (C) and (F) show the normal morphology of the cells by phase contrast microscopy. Scale bar of 25 µm.

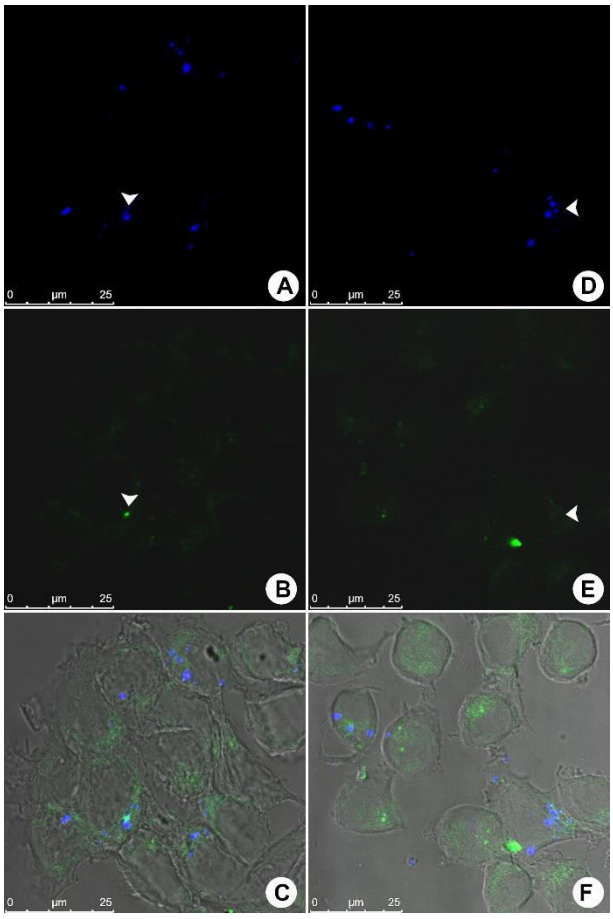

Figure S15. MCF-7 breast cancer cells incubated with **BTD-AO** at 4 °C (A, B and C) and 37 °C (D, E and F) for 15 minutes. The probe accumulated on vesicles (lipid droplets) near to the peripheral region of the cells and at the inner position in the cells. The images show the same result for both temperatures tested as seen in (A), (B), (D) and (E) arrowheads. The blue fluorescent signal is seen in (A) and (D) whereas the green emission is seen in (B) and (E). (C) and (F) show the normal morphology of the cells by phase contrast microscopy. Scale bar of 25 µm.

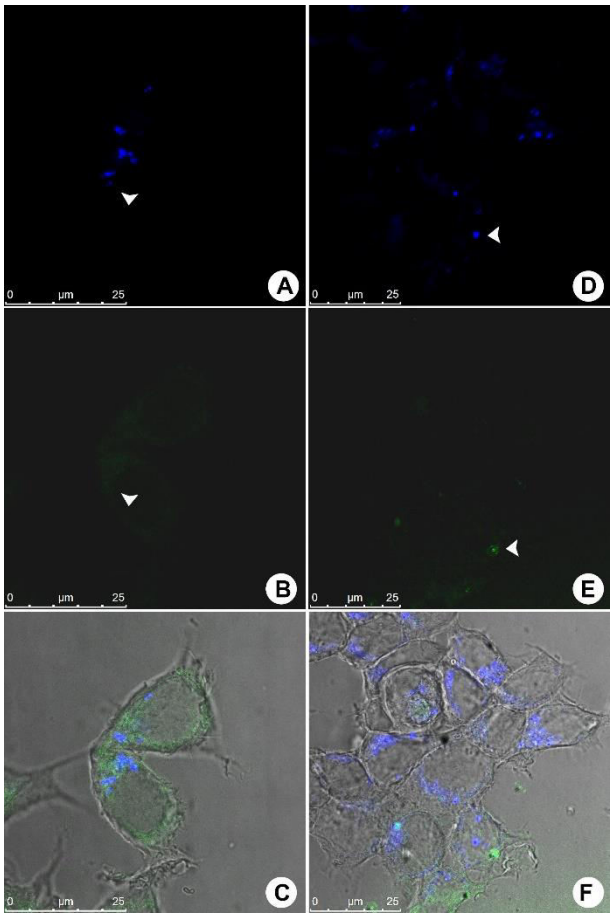

Figure S16. MCF-7 breast cancer cells incubated with **BTD-AO** at 4 °C (A, B and C) and 37 °C (D, E and F) for 30 minutes. The probe accumulated on vesicles (lipid droplets) near to the peripheral region of the cells and at the inner position in the cells. The images show the same result for both temperatures tested as seen in (A), (B), (D) and (E) arrowheads. The blue fluorescent signal is seen in (A) and (D) whereas the green emission is seen in (B) and (E). (C) and (F) show the normal morphology of the cells by phase contrast microscopy. Scale bar of 25 µm.

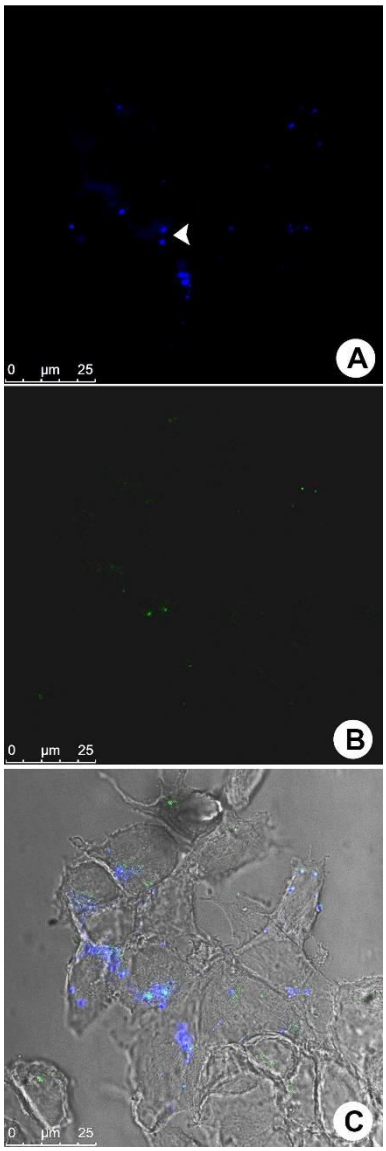

Figure S17. MCF-7 breast cancer cells incubated with **BTD-AO** after 60 min. **BTD-AO** accumulated only inside the lipid droplets (vesicles) and only near to the cell nucleus. (A) Blue emission and (B) Green emission. (C) Shows the normal morphological aspects to these cells by phase contrast microscopy. Scale bar of 25 µm.

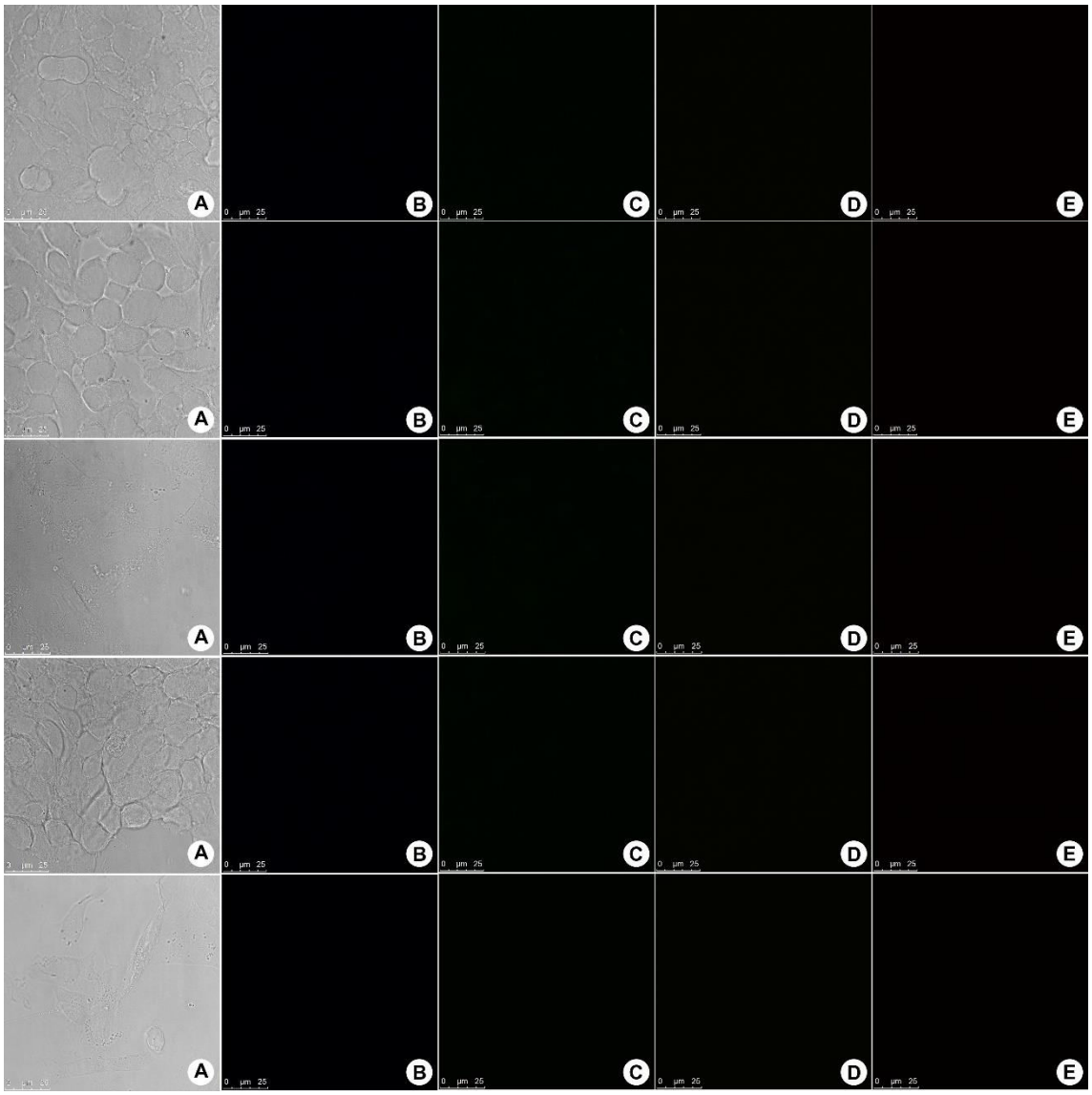

Figure S18. Negative control indicating no autofluorescence of the studied cell models. From top to bottom: MDA-MB-231, MCF-7, Caco-2, HUVEC and HeLa cell lineages. (A) Normal morphological aspects to these cells by phase contrast microscopy. (B) Blue channel. (C) Green channel. (D) Red channel. (E) Overlay of panels (B)-(D). Scale bar of 25 μm.

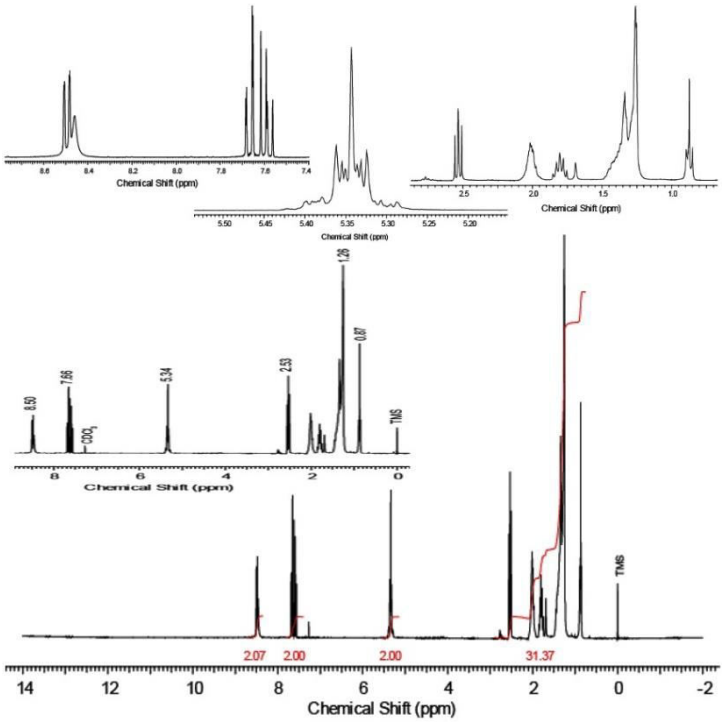

Figure S19. ^{1}H NMR ($CDCl_3$, 300 MHz) of **BTD-AO**.

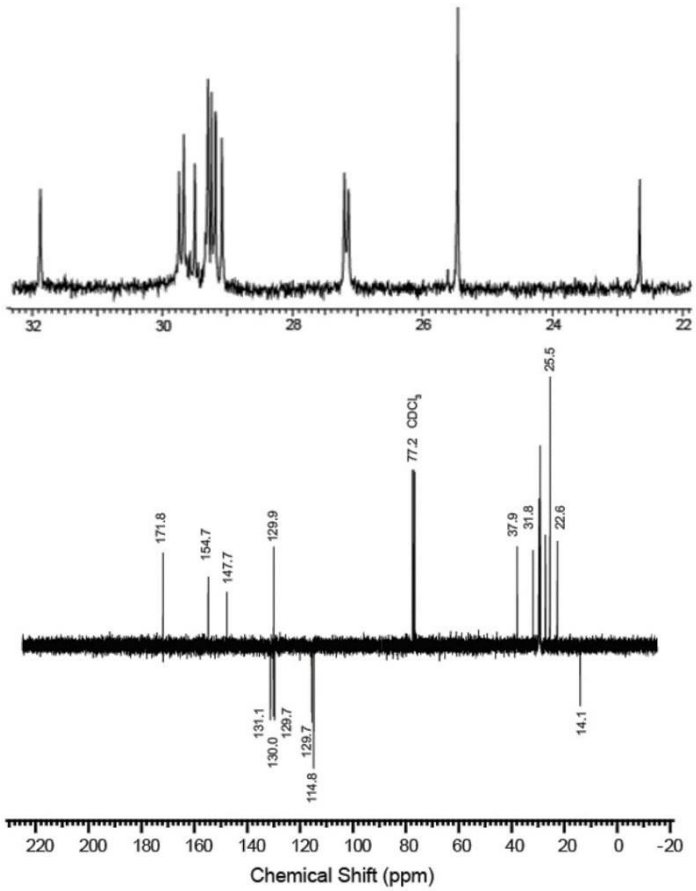

Figure S20. ^{13}C NMR ($CDCl_3$, 75 MHz) of **BTD-AO**.

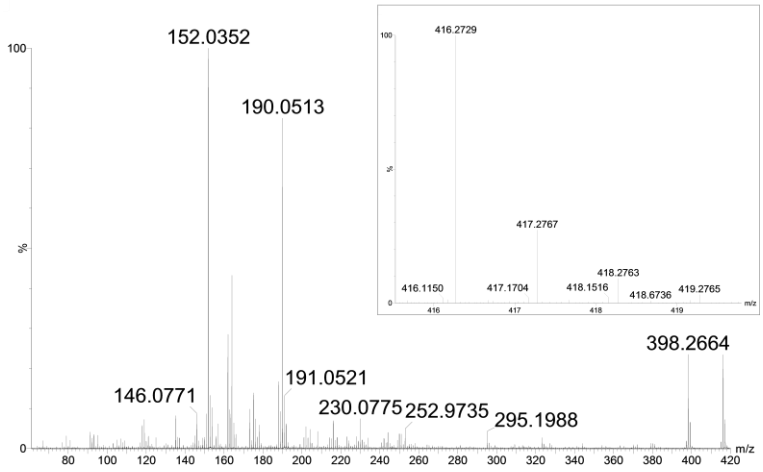

Figure S21. ESI(+)-MS/MS of the protonated **BTD-AO**. The inset is the high resolution ESI(+)-MS with the expected isotopologue composition of the protonated **BTD-AO**. Exact mass calculated for $[C_{24}H_{37}N_3OS + H]^+$ 416.2730. Found 416.2729 (error: -0.24 ppm).

Cartesian coordinates for all the calculated structures (BTD-AO)

S_0 - gas phase

Standard orientation:

Center Number	Atomic Number	Atomic Type	Coordinates (Angstroms) X	Y	Z
1	8	0	-5.085956	-1.716752	1.060126
2	6	0	-4.933108	-0.757224	0.338872
3	6	0	-3.601800	-0.395625	-0.296576
4	7	0	-5.948956	0.112038	0.016670
5	6	0	-2.493419	-1.377534	0.050933
6	6	0	-1.158946	-1.004115	-0.585341
7	6	0	-0.039549	-1.982099	-0.243795
8	6	0	1.299506	-1.615436	-0.875049
9	6	0	2.417859	-2.593704	-0.531855
10	6	0	3.761537	-2.219667	-1.164240
11	6	0	4.834050	-3.227584	-0.874113
12	6	0	5.955203	-3.056718	-0.181398
13	6	0	6.460707	-1.803594	0.469937
14	6	0	7.780639	-1.317792	-0.135982

15	6	0	8.343535	-0.083662	0.560878
16	6	0	9.656825	0.405883	-0.040795
17	6	0	10.220685	1.641048	0.654239
18	6	0	11.533684	2.130938	0.052554
19	6	0	-7.275537	0.061368	0.436191
20	6	0	-7.846938	-0.867016	1.257418
21	6	0	-9.233416	-0.788832	1.603230
22	6	0	-10.065907	0.186081	1.155126
23	6	0	-9.508768	1.173383	0.296345
24	6	0	-8.119259	1.108912	-0.059996
25	7	0	-10.129446	2.209083	-0.255938
26	16	0	-9.034337	3.016296	-1.143008
27	7	0	-7.726181	2.085388	-0.863605
28	1	0	-3.736815	-0.339629	-1.382932
29	1	0	-3.328804	0.617193	0.021889
30	1	0	-5.733894	0.888024	-0.593179
31	1	0	-2.389158	-1.430678	1.137795
32	1	0	-2.791197	-2.381216	-0.264071
33	1	0	-1.272980	-0.951196	-1.675041
34	1	0	-0.868457	0.003999	-0.265073
35	1	0	0.074313	-2.035747	0.845193
36	1	0	-0.329101	-2.989697	-0.564405
37	1	0	1.185592	-1.562378	-1.964607
38	1	0	1.587904	-0.607001	-0.554401
39	1	0	2.538687	-2.651354	0.555248
40	1	0	2.132791	-3.601462	-0.855848
41	1	0	3.629522	-2.146482	-2.250913
42	1	0	4.056106	-1.222596	-0.828307
43	1	0	4.642174	-4.221159	-1.277148
44	1	0	6.612130	-3.918915	-0.074007
45	1	0	5.719093	-1.003143	0.414334
46	1	0	6.616212	-1.998471	1.538317
47	1	0	8.518101	-2.127967	-0.094554
48	1	0	7.628329	-1.105271	-1.199725
49	1	0	7.603441	0.724829	0.522208
50	1	0	8.491284	-0.303526	1.625140
51	1	0	10.397168	-0.402134	-0.001367
52	1	0	9.508791	0.624281	-1.105148
53	1	0	9.480191	2.449069	0.615017

54	1	0	10.368917	1.422513	1.718662
55	1	0	12.275209	1.323717	0.091627
56	1	0	11.386451	2.350013	-1.012025
57	1	0	-7.242486	-1.669645	1.649618
58	1	0	-9.623184	-1.558571	2.259876
59	1	0	-11.112510	0.232332	1.425167
60	6	0	12.098605	3.366395	0.746611
61	1	0	11.358579	4.173487	0.707016
62	1	0	12.246981	3.147661	1.809970
63	6	0	13.410333	3.847438	0.137501
64	1	0	13.286177	4.107587	-0.917158
65	1	0	13.793139	4.731892	0.651460
66	1	0	14.181292	3.074281	0.194419

S_0 – water

Standard orientation:

Center Number	Atomic Number	Atomic Type	Coordinates (Angstroms) X	Y	Z
1	8	0	-5.103870	-1.714044	1.088389
2	6	0	-4.945191	-0.741562	0.375876
3	6	0	-3.608569	-0.360093	-0.228543
4	7	0	-5.963035	0.116994	0.048189
5	6	0	-2.504533	-1.361820	0.072666
6	6	0	-1.165931	-0.952149	-0.532121
7	6	0	-0.048772	-1.947766	-0.237735
8	6	0	1.292687	-1.548774	-0.843789
9	6	0	2.408595	-2.545480	-0.549171
10	6	0	3.752793	-2.142859	-1.162934
11	6	0	4.821479	-3.170445	-0.931074
12	6	0	5.958304	-3.036332	-0.253200
13	6	0	6.487559	-1.813446	0.436911
14	6	0	7.793956	-1.309041	-0.183606
15	6	0	8.385876	-0.112560	0.553724
16	6	0	9.684454	0.396187	-0.063810
17	6	0	10.278840	1.593197	0.671496
18	6	0	11.577224	2.101806	0.053715

19	6	0	-7.296080	0.055445	0.445070
20	6	0	-7.874041	-0.880014	1.255776
21	6	0	-9.265848	-0.818682	1.581094
22	6	0	-10.100733	0.149598	1.120895
23	6	0	-9.538546	1.143270	0.273178
24	6	0	-8.144042	1.095459	-0.061860
25	7	0	-10.161664	2.175024	-0.288234
26	16	0	-9.062317	2.996859	-1.157410
27	7	0	-7.752713	2.079901	-0.858049
28	1	0	-3.734897	-0.243462	-1.310012
29	1	0	-3.336349	0.632317	0.147164
30	1	0	-5.737820	0.897963	-0.552254
31	1	0	-2.402384	-1.473410	1.155681
32	1	0	-2.794635	-2.345966	-0.306960
33	1	0	-1.274541	-0.839477	-1.617334
34	1	0	-0.880727	0.035962	-0.151980
35	1	0	0.061309	-2.057500	0.847660
36	1	0	-0.336847	-2.936453	-0.614334
37	1	0	1.182291	-1.440065	-1.929393
38	1	0	1.580851	-0.559601	-0.468282
39	1	0	2.527552	-2.654763	0.534581
40	1	0	2.121483	-3.534696	-0.924457
41	1	0	3.616324	-2.013712	-2.243767
42	1	0	4.051971	-1.166429	-0.774965
43	1	0	4.613345	-4.145505	-1.370452
44	1	0	6.610023	-3.907322	-0.192598
45	1	0	5.749675	-1.007873	0.434874
46	1	0	6.673618	-2.055310	1.490562
47	1	0	8.525758	-2.125165	-0.199843
48	1	0	7.613243	-1.042803	-1.231045
49	1	0	7.650785	0.701005	0.573953
50	1	0	8.564216	-0.385044	1.600917
51	1	0	10.419138	-0.417776	-0.083766
52	1	0	9.505416	0.667125	-1.111272
53	1	0	9.544151	2.407223	0.691520
54	1	0	10.458049	1.322402	1.719039
55	1	0	12.312952	1.288535	0.033748
56	1	0	11.399035	2.372915	-0.994067
57	1	0	-7.272264	-1.679029	1.657688

58	1	0	-9.657818	-1.593543	2.229866
59	1	0	-11.151681	0.181364	1.376432
60	6	0	12.172839	3.299311	0.787534
61	1	0	11.438698	4.112518	0.806992
62	1	0	12.351778	3.028982	1.834222
63	6	0	13.469879	3.798999	0.161732
64	1	0	13.314977	4.108657	-0.875506
65	1	0	13.875134	4.655958	0.704669
66	1	0	14.234915	3.017669	0.159891

S_1 – gas phase

Standard orientation:

Center Number	Atomic Number	Atomic Type	Coordinates (Angstroms) X	Y	Z
1	8	0	-5.116220	-1.790525	1.062690
2	6	0	-4.938786	-0.823319	0.367755
3	6	0	-3.614775	-0.450576	-0.258750
4	7	0	-5.964363	0.079712	0.059263
5	6	0	-2.501050	-1.430466	0.077636
6	6	0	-1.171308	-1.042445	-0.560072
7	6	0	-0.045599	-2.017005	-0.229742
8	6	0	1.288812	-1.636896	-0.862891
9	6	0	2.413776	-2.611298	-0.530502
10	6	0	3.752991	-2.225131	-1.164930
11	6	0	4.831805	-3.229294	-0.885105
12	6	0	5.954737	-3.056440	-0.195816
13	6	0	6.456800	-1.804659	0.460638
14	6	0	7.772517	-1.310005	-0.147350
15	6	0	8.332776	-0.077313	0.554177
16	6	0	9.642060	0.420477	-0.049446
17	6	0	10.203653	1.654081	0.650189
18	6	0	11.512785	2.151897	0.046590
19	6	0	-7.267727	0.070361	0.438340
20	6	0	-7.879970	-0.916050	1.271023
21	6	0	-9.215774	-0.797499	1.574442
22	6	0	-9.994825	0.271184	1.085204
23	6	0	-9.415044	1.261058	0.259467

24	6	0	-8.042296	1.155509	-0.063213
25	7	0	-10.029725	2.319423	-0.269858
26	16	0	-8.859979	3.140543	-1.152009
27	7	0	-7.546633	2.111664	-0.842303
28	1	0	-3.754508	-0.380814	-1.344018
29	1	0	-3.351464	0.562166	0.068665
30	1	0	-5.737607	0.873585	-0.534532
31	1	0	-2.391884	-1.491797	1.163768
32	1	0	-2.793765	-2.432762	-0.246526
33	1	0	-1.289656	-0.981376	-1.648631
34	1	0	-0.886344	-0.035570	-0.231907
35	1	0	0.072703	-2.078486	0.858337
36	1	0	-0.330106	-3.023626	-0.557748
37	1	0	1.170856	-1.576394	-1.951532
38	1	0	1.572159	-0.629323	-0.535432
39	1	0	2.538890	-2.675913	0.555722
40	1	0	2.133359	-3.618312	-0.860785
41	1	0	3.616911	-2.145082	-2.250589
42	1	0	4.043263	-1.228909	-0.822898
43	1	0	4.643756	-4.221273	-1.293794
44	1	0	6.616641	-3.915763	-0.096534
45	1	0	5.711633	-1.007025	0.412058
46	1	0	6.617011	-2.004792	1.527336
47	1	0	8.513463	-2.117288	-0.112869
48	1	0	7.615579	-1.092406	-1.209380
49	1	0	7.589409	0.728469	0.522267
50	1	0	8.485076	-0.302209	1.616741
51	1	0	10.385602	-0.384893	-0.016876
52	1	0	9.489482	0.643955	-1.112091
53	1	0	9.460086	2.459570	0.617696
54	1	0	10.356346	1.430528	1.712938
55	1	0	12.257359	1.347194	0.078901
56	1	0	11.361103	2.376014	-1.016305
57	1	0	-7.280534	-1.731649	1.643019
58	1	0	-9.683042	-1.543285	2.205276
59	1	0	-11.045849	0.345429	1.336650
60	6	0	12.075594	3.385757	0.745193
61	1	0	11.332550	4.190369	0.712302
62	1	0	12.228381	3.162025	1.806886

63	6	0	13.383489	3.874678	0.134135
64	1	0	13.254774	4.140009	-0.918676
65	1	0	13.764887	4.757744	0.651487
66	1	0	14.157394	3.104004	0.184304

S_1 – water

Standard orientation:

Center Number	Atomic Number	Atomic Type	Coordinates (Angstroms) X	Y	Z
1	8	0	-5.181828	-1.852635	0.956525
2	6	0	-4.981315	-0.828203	0.350544
3	6	0	-3.639180	-0.392518	-0.179646
4	7	0	-6.009048	0.086424	0.070921
5	6	0	-2.535050	-1.403347	0.089102
6	6	0	-1.189918	-0.955173	-0.472245
7	6	0	-0.072977	-1.959818	-0.209615
8	6	0	1.272495	-1.532393	-0.786667
9	6	0	2.388263	-2.537702	-0.522319
10	6	0	3.733742	-2.114710	-1.119076
11	6	0	4.802532	-3.148130	-0.915448
12	6	0	5.948170	-3.027415	-0.250037
13	6	0	6.491128	-1.816167	0.449871
14	6	0	7.788215	-1.305812	-0.185278
15	6	0	8.395089	-0.120295	0.557543
16	6	0	9.684210	0.393405	-0.075561
17	6	0	10.293615	1.580405	0.663621
18	6	0	11.582493	2.093427	0.029748
19	6	0	-7.324603	0.029631	0.384849
20	6	0	-7.956444	-1.038125	1.100106
21	6	0	-9.301545	-0.979382	1.355802
22	6	0	-10.096039	0.112172	0.932580
23	6	0	-9.509814	1.180357	0.226733
24	6	0	-8.110944	1.140607	-0.050669
25	7	0	-10.127278	2.269486	-0.233166
26	16	0	-8.949410	3.201751	-0.991622
27	7	0	-7.624386	2.175030	-0.716579
28	1	0	-3.738495	-0.204577	-1.254372

29	1	0	-3.393620	0.577272	0.267545
30	1	0	-5.749963	0.924236	-0.441586
31	1	0	-2.450468	-1.569200	1.166763
32	1	0	-2.813978	-2.367179	-0.346160
33	1	0	-1.282590	-0.789694	-1.551976
34	1	0	-0.916732	0.013875	-0.038596
35	1	0	0.027511	-2.115356	0.871017
36	1	0	-0.354866	-2.932062	-0.630854
37	1	0	1.171168	-1.380707	-1.867957
38	1	0	1.554413	-0.558390	-0.369258
39	1	0	2.504061	-2.683235	0.557490
40	1	0	2.102705	-3.513854	-0.931469
41	1	0	3.600086	-1.952814	-2.195910
42	1	0	4.030875	-1.150281	-0.700752
43	1	0	4.586619	-4.115645	-1.367621
44	1	0	6.598033	-3.901027	-0.211237
45	1	0	5.755353	-1.008961	0.471606
46	1	0	6.694094	-2.073876	1.496598
47	1	0	8.517886	-2.123055	-0.224541
48	1	0	7.590667	-1.025396	-1.225949
49	1	0	7.662360	0.694508	0.600597
50	1	0	8.590474	-0.406635	1.597968
51	1	0	10.416684	-0.421705	-0.117658
52	1	0	9.488113	0.677179	-1.116549
53	1	0	9.561238	2.395675	0.705589
54	1	0	10.489944	1.296978	1.704731
55	1	0	12.316010	1.278976	-0.011805
56	1	0	11.387198	2.376646	-1.011763
57	1	0	-7.357774	-1.872839	1.425450
58	1	0	-9.772780	-1.789783	1.896706
59	1	0	-11.156973	0.131618	1.148851
60	6	0	12.193053	3.281431	0.766686
61	1	0	11.461156	4.095859	0.807584
62	1	0	12.389065	2.999088	1.807123
63	6	0	13.480437	3.785407	0.124575
64	1	0	13.308717	4.106780	-0.906433
65	1	0	13.896673	4.635520	0.669955
66	1	0	14.243626	3.002620	0.101219

REFERENCES

1. Frisch, M. J., Trucks, G. W., Schlegel, H. B., Scuseria, G. E., Robb, M. A., Cheeseman, J. R., Scalmani, G., Barone, V., Mennucci, B., Petersson, G. A., Nakatsuji, H., Caricato, M., Li, X., Hratchian, H. P., Izmaylov, A. F., Bloino, J., Zheng, G., Sonnenberg, J. L., Hada, M., Ehara, M., Toyota, K., Fukuda, R., Hasegawa, J., Ishida, M., Nakajima, T., Honda, Y., Kitao, O., Nakai, H., Vreven, T., Montgomery, J. A., Peralta, J. E., Ogliaro, F., Bearpark, M., Heyd, J. J., Brothers, E., Kudin, K. N., Staroverov, V. N., Kobayashi, R., Normand, J., Raghavachari, K., Rendell, A., Burant, J. C., Iyengar, S. S., Tomasi, J., Cossi, M., Rega, N., Millam, J. M., Klene, M., Knox, J. E., Cross, J. B., Bakken, V., Adamo, C., Jaramillo, J., Gomperts, R., Stratmann, R. E., Yazyev, O., Austin, A. J., Cammi, R., Pomelli, C., Ochterski, J. W., Martin, R. L., Morokuma, K., Zakrzewski, V. G., Voth, G. A., Salvador, P., Dannenberg, J. J., Dapprich, S., Daniels, A. D., Farkas, Foresman, J. B., Ortiz, J. V., Cioslowski, J., and Fox, D. J. (2009) Gaussian 09, Revision A.02, Wallingford CT.
2. T. Yanai, D. Tew, and N. Handy, "A new hybrid exchange-correlation functional using the Coulomb-attenuating method (CAM-B3LYP)," Chem. Phys. Lett., 393 (2004) 51-57
3. Fonseca, T. L., de Oliveira, H. C. B., and Castro, M. A. (2008) Theoretical study of the lowest electronic transitions of sulfur-bearing mesoionic compounds in gas-phase and in dimethyl sulfoxide, *Chem. Phys. Lett. 457*, 119-123.
4. Miertus, S., Scrocco, E., and Tomasi, J. (1981) Electrostatic interaction of a solute with a continuum - a direct utilization of abinitio molecular potentials for the prevision of solvent effects, *Chem. Phys. 55*, 117-129.
5. Cammi, R., and Tomasi, J. (1995) Remarks on the use of the apparent surface-charges (asc) methods in solvation problems - iterative versus matrix-inversion procedures and the renormalization of the apparent charges, *J. Comput. Chem. 16*, 1449-1458.
6. Tomasi, J., Mennucci, B., and Cammi, R. (2005) Quantum mechanical continuum solvation models, *Chem Rev 105*, 2999-3093.
7. M. J. Frisch, G. W. Trucks, H. B. Schlegel, G. E. Scuseria, M. A. Robb, J. R. Cheeseman, G. Scalmani, V. Barone, B. Mennucci, G. A. Petersson, H. Nakatsuji, M. Caricato, X. Li, H. P. Hratchian, A. F. Izmaylov, J. Bloino, G. Zheng, J. L. Sonnenberg, M. Hada, M. Ehara, K. Toyota, R. Fukuda, J. Hasegawa, M. Ishida, T. Nakajima, Y. Honda, O. Kitao, H. Nakai, T. Vreven, J. A.

Montgomery, J. E. Peralta, F. Ogliaro, M. Bearpark, J. J. Heyd, E. Brothers, K. N. Kudin, V. N. Staroverov, R. Kobayashi, J. Normand, K. Raghavachari, A. Rendell, J. C. Burant, S. S. Iyengar, J. Tomasi, M. Cossi, N. Rega, J. M. Millam, M. Klene, J. E. Knox, J. B. Cross, V. Bakken, C. Adamo, J. Jaramillo, R. Gomperts, R. E. Stratmann, O. Yazyev, A. J. Austin, R. Cammi, C. Pomelli, J. W. Ochterski, R. L. Martin, K. Morokuma, V. G. Zakrzewski, G. A. Voth, P. Salvador, J. J. Dannenberg, S. Dapprich, A. D. Daniels, Farkas, J. B. Foresman, J. V. Ortiz, J. Cioslowski and D. J. Fox, Wallingford CT, 2009.

8. T. L. Fonseca, H. C. B. de Oliveira and M. A. Castro, *Chem. Phys. Lett.*, 2008, **457**, 119-123.
9. N. L. Marana, V. M. Longo, E. Longo, J. B. L. Martins and J. R. Sambrano, *J. Phys. Chem. A*, 2008, **112**, 8958-8963.
10. S. Miertus, E. Scrocco and J. Tomasi, *Chem. Phys.*, 1981, **55**, 117-129.
11. R. Cammi and J. Tomasi, *J. Comput. Chem.*, 1995, **16**, 1449-1458.
12. J. Tomasi, B. Mennucci and R. Cammi, *Chem. Rev.*, 2005, **105**, 2999-3093.
13. S. Curry, H. Mandelkow, P. Brick and N. Franks, *Nat Struct Biol*, 1998, **5**, 827-835.
14. C. Lucke, Y. Qiao, H. T. van Moerkerk, J. H. Veerkamp and J. A. Hamilton, *Biochemistry*, 2006, **45**, 6296-6305.
15. P. J. Goodford, *J. Med. Chem.*, 1985, **28**, 849-857.
16. S. J. Weiner, P. A. Kollman, D. T. Nguyen and D. A. Case, *J. Comp. Chem.*, 1986, **7**, 230-252.
17. G. M. Morris, D. S. Goodsell, R. S. Halliday, R. Huey, W. E. Hart, R. K. Belew and A. J. Olson, *J. Comp. Chem.*, 1998, **19**, 1639-1662.
18. R. Huey, G. M. Morris, A. J. Olson and D. S. Goodsell, *J. Comp. Chem.*, 2007, **28**, 1145-1152.
19. G. M. Morris, R. Huey, W. Lindstrom, M. F. Sanner, R. K. Belew, D. S. Goodsell and A. J. Olson, *J. Comp. Chem.*, 2009, **30**, 2785-2791.